Since January 2020 Elsevier has created a COVID-19 resource centre with free information in English and Mandarin on the novel coronavirus COVID-19. The COVID-19 resource centre is hosted on Elsevier Connect, the company's public news and information website.

ACADEMIC PRESS

Available online at www.sciencedirect.com

SCIENCE DIRECT®

VIROLOGY

Virology 312 (2003) 369–380

www.elsevier.com/locate/yviro

Amino acid substitutions within the heptad repeat domain 1 of murine coronavirus spike protein restrict viral antigen spread in the central nervous system

Jean C. Tsai,[a] Linda de Groot,[a] Josefina D. Pinon,[a] Kathryn T. Iacono,[a] Joanna J. Phillips,[a] Su-hun Seo,[a] Ehud Lavi,[b] and Susan R. Weiss[a,*]

[a] *Department of Microbiology, University of Pennsylvania School of Medicine, Philadelphia, PA 19104-6076, USA*
[b] *Department of Pathology and Laboratory Medicine, University of Pennsylvania School of Medicine, Philadelphia, PA 19104-6076, USA*

Received 18 December 2002; returned to author for revision 25 February 2003; accepted 7 March 2003

Abstract

Targeted recombination was carried out to select mouse hepatitis viruses (MHVs) in a defined genetic background, containing an MHV-JHM spike gene encoding either three heptad repeat 1 (HR1) substitutions (Q1067H, Q1094H, and L1114R) or L1114R alone. The recombinant virus, which expresses spike with the three substitutions, was nonfusogenic at neutral pH. Its replication was significantly inhibited by lysosomotropic agents, and it was highly neuroattenuated in vivo. In contrast, the recombinant expressing spike with L1114R alone mediated cell-to-cell fusion at neutral pH and replicated efficiently despite the presence of lysosomotropic agents; however, it still caused only subclinical morbidity and no mortality in animals. Thus, both recombinant viruses were highly attenuated and expressed viral antigen which was restricted to the olfactory bulbs and was markedly absent from other regions of the brains at 5 days postinfection. These data demonstrate that amino acid substitutions, in particular L1114R, within HR1 of the JHM spike reduced the ability of MHV to spread in the central nervous system. Furthermore, the requirements for low pH for fusion and viral entry are not prerequisites for the highly attenuated phenotype.

Keywords: Murine coronavirus; Viral pathogenesis; CNS infection; MHV spike; Viral fusion

Introduction

The spike glycoprotein, found on the virion envelope of the coronavirus mouse hepatitis virus (MHV), is a major determinant of viral pathogenicity (Phillips et al., 1999). Entry into susceptible cells and cell-to-cell spread of MHV are mediated by the spike. Spike is synthesized as an 180- to 220-kDa glycosylated precursor that is posttranslationally cleaved into two 90-kDa subunits, S1 and S2 (Frana et al., 1985). Oligomeric spike is present on both viral and infected cell membranes. The receptor binding domain (RBD) of spike has been mapped to the amino-terminal 330 amino acid residues of the S1 subunit (Kubo et al., 1994), which is though to form the globular head of the spike. The RBD is responsible for the initial attachment of MHV to the cell-surface receptors, members of the CEACAM subclass of the CEA gene family (Dveksler et al., 1991). This initial binding event is thought to trigger a conformational change in spike that allows S2, the stalk portion of the peplomer, to initiate fusion of the two membranes (Gallagher and Buchmeier, 2001; Matsuyama and Taguchi, 2002a; Zelus et al., 2003). A candidate fusion peptide domain has been identified within S2 (Luo and Weiss, 1998; Fig. 1); however, the actual fusion peptide for the MHV spike has not been definitively identified. Within S2 there are two heptad repeat (HR) domains (HR1 and HR2) which are structural features common to all coronavirus spikes as well as of

* Corresponding author. Department of Microbiology, 203A Johnson Pavilion, University of Pennsylvania, Philadelphia, PA 19104-6076. Fax: +1-215-573-4858.
E-mail address: weisssr@mail.med.upenn.edu (S.R. Weiss).

0042-6822/03/$ – see front matter © 2003 Elsevier Science (USA). All rights reserved.
doi:10.1016/S0042-6822(03)00248-4

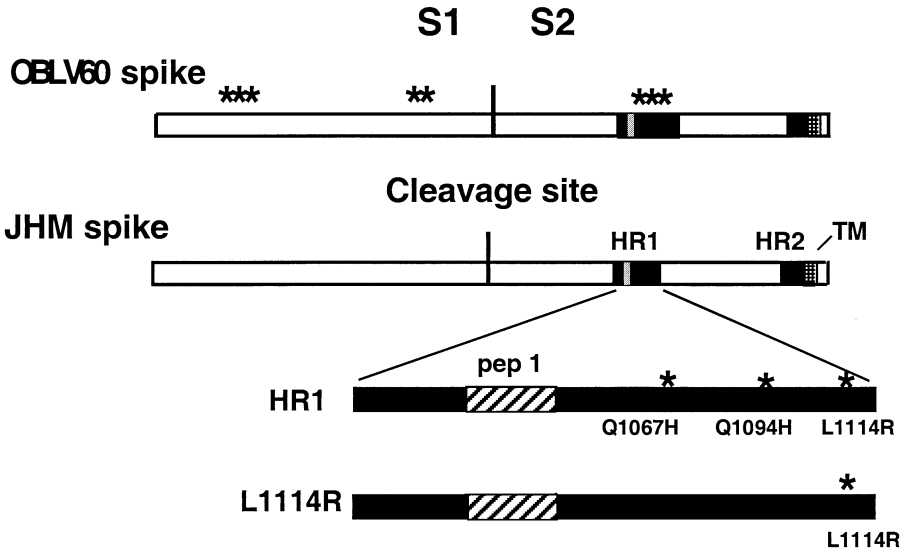

Fig. 1. Schematic diagram of wild-type and mutant JHM spike proteins. The OBL V60 spike is shown with asterisks marking the positions of the eight amino acid substitutions within the spike (from amino to carboxyl ends—K107R, N134T, L141F, D597N, Q600K, Q1067H, Q1094H, L1114R) (from Gallagher et al., 1991). Also shown is the JHM spike, with the locations of the cleavage site represented by the vertical line separating the S1 and S2 subunits, as well as the heptad repeat (HR) and transmembrane (TM) domains. The HR1 is enlarged to show the locations of the amino acid substitutions in the mutant proteins containing either three substitutions in HR1 (HR1) or L1114R alone; a candidate fusion peptide (pep1; Luo and Weiss, 1998) within HR1 is also indicated.

attachment/fusion proteins of many other viruses (DeGroot et al., 1987). More recently, a third heptad repeat region located to the N-terminal side of HR1 was predicted within the MHV spike (Gallagher and Buchmeier, 2001; Krueger et al., 2001). The HR domains are believed to form α-helical configurations, which have been though to play a role in the oligomerization of the spike peplomer (DeGroot et al., 1987; Luo et al., 1999). It has also been believed that these domains participate in the conformational change of the spike peplomer, which allows for the insertion of the putative fusion peptide into the cell membrane and that interactions between HR1 and RBD may play a role in fusion (Krueger et al., 2001; Matsuyama and Taguchi, 2002b). However, recently, it has been shown that the S1 subunit contains sequences responsible for oligomerization (Lewicki and Gallagher, 2003), suggesting that the conformational changes that spike undergoes during the process of fusion may be quite different from previously postulated.

The entry route for MHV has not been clearly defined. Previous studies have demonstrated that the wild-type JHM strain (previously referred to as MHV-4; see Materials and methods) can utilize both endosomal and nonendosomal pathways for entry (Nash and Buchmeier, 1997). Wild-type JHM fuses at neutral pH; however, persistent JHM infection of a neuronal cell line (OBL21a) gave rise to an acid-dependent fusion variant OBLV60. OBLV60 is unable to induce fusion at neutral pH and enters cells via the endosomal route (Gallagher et al., 1991; Nash and Buchmeier, 1997). Sequencing of the spike genes of JHM and OBLV60 demonstrated that there were eight amino acid differences between these two spike proteins. Five of these substitutions were located in the S1 subunit of the spike gene. However, it was demonstrated that the change from neutral pH-induced fusion to low pH-induced fusion was dependent on the amino acid substitutions Q1067H, Q1094H, and L1114R, all within the first heptad repeat (HR1) of the S2 subunit (Gallagher et al., 1991; see Fig. 1).

JHM is a highly neurovirulent MHV strain (Dalziel et al., 1986; Gallagher et al., 1991); following infection of susceptible weanling mice with JHM, there is widespread distribution of infection in the brain, often resulting in fatal encephalitis. In contrast, the OBLV60 variant is neuroattenuated; infection with OBLV60 is limited mainly to the neurons of the mitral and glomerular layers of the olfactory bulbs, and no fatal encephalitis is observed (Pearce et al., 1994). We wanted to determine whether the three amino acid substitutions in the HR1 of the OBLV60 spike were responsible for its low pH-dependent route of entry into cells in vitro and/or the attenuation and limited spread of the virus in vivo. It was also important to determine whether these phenotypes could be dissociated from each other. We were particularly interested in the substitution at residue L1114, as this residue has been substituted in viruses with altered phenotypes isolated in several studies (Gallagher et al., 1991; Wang et al., 1992; Saeki et al., 1997).

We have previously used targeted RNA recombination to demonstrate the important role spike plays as a major determinant of pathogenicity in the central nervous system (CNS) (Phillips et al., 1999). Subsequently we used recombinant viruses expressing chimeric spike proteins to demonstrate that the RBD determines the specificity of receptor utilization (Tsai et al., 2003). Here we focus on the phenotype of a virus encoding the three HR1 amino acids that were previously shown to be sufficient to result in the low

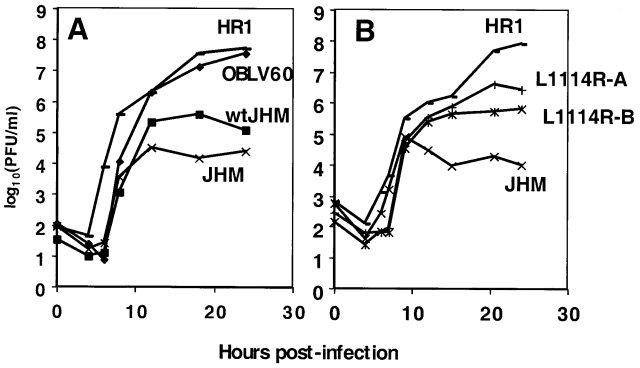

Fig. 2. Replication of wild-type and mutant viruses in L2 cell culture. L2 cells were infected in duplicate at an m.o.i. of 2 PFU/cell. At the indicated times postinfection, cells were lysed and virus titered by plaque assay. Each point represents the logarithmic mean titer of duplicate samples. (A) Cells were infected wild-type JHM virus (wtJHM), OBLV60, or recombinant viruses SJHM-RA59, expressing wild-type JHM spike (JHM) or SJHM-HR1, expressing the JHM spike with three HR1 substitutions (HR1). (B) Cells were infected with the following recombinant viruses: SJHM-RA59 (JHM); SJHM-HR1 (HR1); or two independent isolates of SJHM-L1114R, expressing JHM spike with the L1114R substitution (L1114R-A; L1114R-B).

pH-dependent requirement for cell-to-cell fusion (Gallagher et al., 1991). Thus, we have selected recombinant viruses with a defined genetic background expressing the JHM spike protein, encoding the amino acid substitutions in HR1 of OBLV60 (Q1067H, Q1094H, and L1114R) or L1114 alone. The three substitutions are sufficient to confer a neuroattenuated phenotype to this recombinant virus, which similar to OBLV60, displays virus spread restricted to the olfactory bulbs. Interestingly the L1114R substitution alone is capable of causing in vivo attenuation and restricted spread, while displaying a fusion phenotype close to wild-type as well as the ability to enter cells at neutral pH.

Results

Selection and in vitro phenotypes of recombinant viruses with amino acid substitutions in the HR1 of the spike protein

We wanted to determine whether the three mutations in HR1 of the JHM spike, Q1067H, Q1094H, and L1114R, were sufficient to cause in vivo attenuation and restriction of antigen to the olfactory bulbs. If so, we then wanted to determine whether these in vivo phenotypes were dependent on the in vitro property of acid pH-dependent fusion and entry (Gallagher et al., 1991; Nash and Buchmeier, 1997). This was not possible to accomplish with OBLV60, due to the presence of five other substitutions within S1 (Fig. 1) and an unknown number of amino acid substitutions outside of the spike. Thus, we used targeted RNA recombination to select isogenic recombinant viruses expressing the JHM spike gene encoding either the three HR1 amino acid substitutions (SJHM-HR1) or the L1114R alone (SJHM-L1114R), as well as a virus expressing wild-type JHM spike (SJHM-RA59) (Kuo et al., 2000; Phillips et al., 2001). (See Fig. 1 for a schematic of the spike proteins expressed by these viruses.) All these viruses had genes other than spike derived from MHV-A59 (Phillips et al., 1999) and are described under Materials and methods.

SJHM-RA59 replicates to relatively low titers in mouse L2 fibroblasts in vitro, similar to wild-type JHM (Phillips et al., 1999, 2001). Compared to JHM or SJHM-RA59 viruses, OBLV60 and SJHM-HR1 replicated to much higher titers while SJHM-L1114R replicated to titers intermediate between those of SJHM-RA59 and SJHM-HR1 (Fig. 2). The replication characteristics of OBLV60, SJHM-HR1, JHM, and SJHM-RA59 in OBL21a cells were similar to those in L2 cells (data not shown).

An in vitro fusion assay was performed to compare the levels of cell-to-cell fusion induced by recombinant viruses SJHM-RA59, SJHM-HR1, and SJHM-L1114R. As shown in Fig. 3, SJHM-HR1 lacks the ability to induce cell-to-cell fusion at neutral pH. This is consistent with previous data on the inability of OBLV60 to induce cell-to-cell fusion at neutral pH (Gallagher et al., 1991) and confirms the observation that the three amino acid substitutions in HR1 (Q1067H, Q1094H, and L1114R) present in both SJHM-HR1 and OBLV60 are sufficient to confer a fusion-negative phenotype at neutral pH. SJHM-L1114R, expressing the L1114R substitution alone, does induce significant levels of cell-to-cell fusion at neutral pH; however, fusion induced by this recombinant is less extensive than that induced by SJHM-RA59 (Fig. 3). Thus, the L1114R substitution is not sufficient to confer the nonfusogenic phenotype of SJHM-HR1.

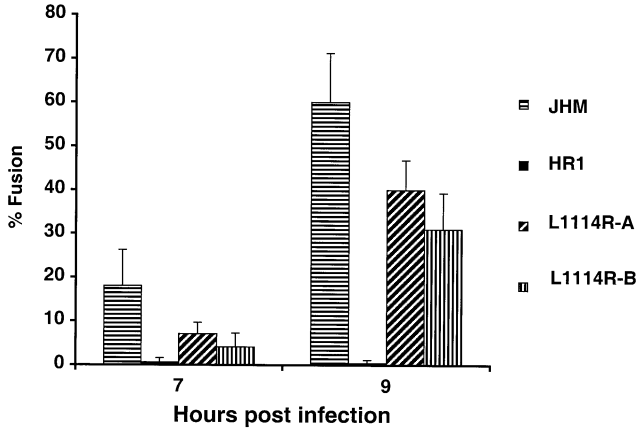

Fig. 3. Virus-induced cell-to-cell fusion of L2 cells. L2 cell monolayers were infected in duplicate at an m.o.i. of 1 PFU/cell with recombinant viruses expressing either wild-type or mutant spike proteins. At 7 and 9 h postinfection, the cells were fixed and visualized at ×200 magnification using phase-contrast microscopy. Fusion expressed as the mean percentage of nuclei in syncytium is plotted with the error bar representing the standard deviation.

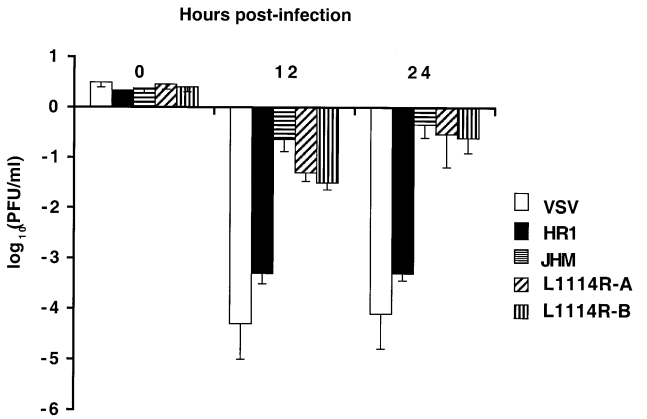

Fig. 4. Effect of lysosomotropic agents on viral replication in L2 cells. L2 cell monolayers were treated for 1 h with 20 mM ammonium chloride and then infected with either vesicular stomatitis virus (VSV) or recombinant MHVs expressing wild-type or mutant spikes as indicated. The presence of 20 mM ammonium chloride was continuous throughout the infection. At 0, 12, and 24 h postinfection, the level of infectious titer was measured by plaque assay and expressed as the difference between logarithmic mean ($\Delta \log_{10}$(PFU/ml)) titer of the treated and untreated samples (four independent samples per virus). The error bars represent the standard deviations.

To determine whether, similar to OBLV60, the mutant recombinant viruses rely on the acidification of the endosomal vesicles to trigger fusion, we tested the effects of the lysosomotropic agent, ammonium chloride, on the replication of SJHM-RA59, SJHM-HR1, and SJHM-L1114R in vitro (Fig. 4). Vesicular stomatitis virus (VSV), which is known to enter cells via the endosomal pathway and to require low pH for entry, was used as a control. In the presence of 20 mM ammonium chloride, the replication of VSV was reduced about 10,000-fold at 12 and 24 h postinfection of L2 cells (Fig. 4). Similarly, the replication of SJHM-HR1 was reduced more than 1000-fold in the presence of 20 mM ammonium chloride. Similar levels of inhibition were observed for OBLV60 (Gallagher et al., 1991; our data, not shown). In contrast, only a minimal reduction in replication level was observed when either SJHM-RA59 or SJHM-L1114R infection of L2 cells was carried in the presence of ammonium chloride. (Statistical analysis demonstrated, however, that SJHM-L1114R was inhibited to a greater extent than SJHM-RA59.) Similar patterns of inhibition were observed in infections carried out in the presence of 40 μM chloroquine (data not shown). Thus, the L1114R substitution alone does not result in an absolute dependence on low pH for virus entry.

Recombinant viruses with HR1 mutations are neuroattenuated and restricted in spread in the brain despite efficient replication

Wild-type JHM or recombinant viruses encoding the JHM spike (SJHM-RA59) are highly neurovirulent and disseminate throughout the murine brain, often causing mortality (Lavi et al., 1990; Barnett et al., 1993; Phillips et al., 1999). OBLV60 is a highly neuroattenuated mutant of JHM (Pearce et al., 1994). To determine whether the three amino acid substitutions in the HR1 of OBLV60 or L1114R alone are sufficient to confer a neuroattenuated phenotype, mice were inoculated either intracranially (ic) or intranasally (in) with serial dilutions of SJHM-RA59, SJHM-HR1, and SJHM-L1114R and observed for disease and death. Inoculation with SJHM-HR1 (up to 5000 PFU ic and up to 10^5 PFU in) or with SJHM-L1114R (up to 10^4 PFU ic) did not result in any mortality throughout the 21 to 28 days the mice were observed. In contrast, mice inoculated with doses as low as 1 PFU ic or 1000 PFU in of SJHM-RA59 exhibited clinical signs of disease, such as hunched posture, ruffled fur, and abnormal gait with occasional paralysis, at 4–5 days postinfection. Thus, recombinant viruses expressing either all three HR1 substitutions or L1114R alone induced clinically silent infections and are basically avirulent. Even L1114R alone is sufficient to highly attenuate MHV.

To begin to understand the mechanism of the attenuation of SJHM-HR1 and SJHM-L1114R, we examined the ability of these viruses to replicate and express viral antigen in the brain. We used the in route of inoculation because it is a more natural route and detection of viral antigen following in inoculation is more discreet than following ic inoculation. Thus, mice were inoculated in with 5000 PFU each of SJHM-RA59, SJHM-HR1, or SJHM-L1114R and titers of infectious virus in the brain at various times postinfection were determined by plaque titration. Patterns of infection with all of these viruses were similar in terms of kinetics and extent of replication; viral replication in the brain peaked at 5 days postinfection (Fig. 5). SJHM-HR1 displayed slightly higher viral titers at 5 and 7 days postinfection as compared to SJHM-RA59; however, the difference

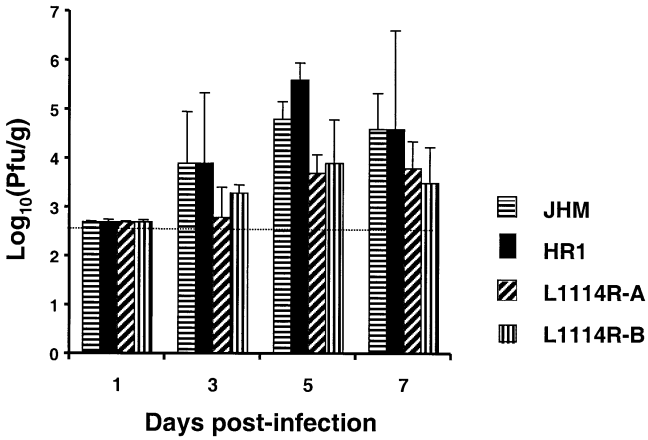

Fig. 5. Replication of virus in brains of infected mice. Four-week-old C57B1/6 mice were inoculated intranasally with 5000 PFU of recombinant viruses expressing wild-type or mutant JHM spikes as indicated. At the indicated times, mice (three per time point) were sacrificed and brains harvested and homogenized. Viral titers were determined by plaque assay of brain homogenates and expressed as the logarithmic mean titer per gram of tissue homogenate. The standard deviations of the mean are plotted as error bars. The limit of detection of this assay was 2.7 $\log_{10}$(PFU/g).

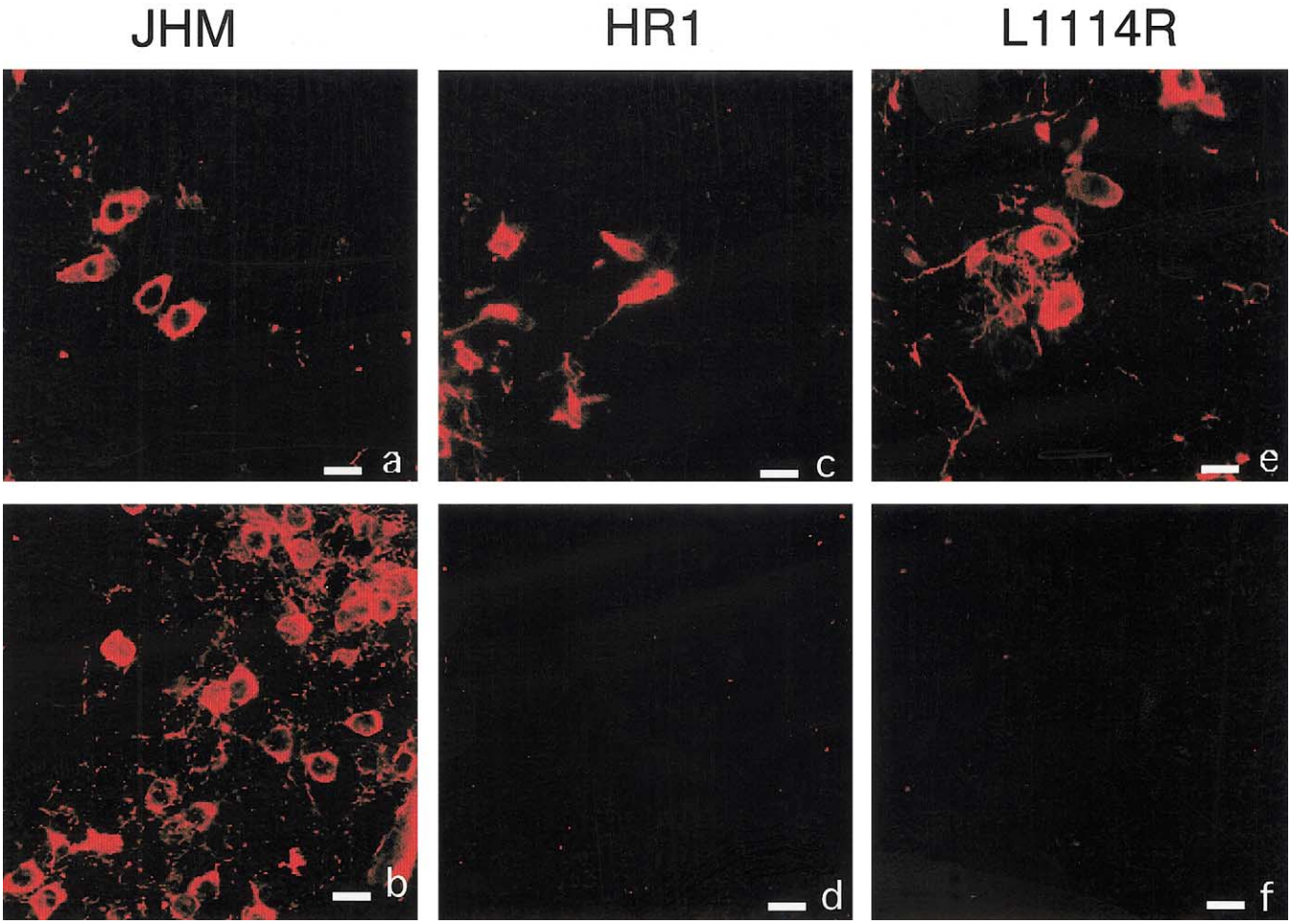

Fig. 6. Viral antigen distribution in the brains of infected mice. Indirect immunofluorescent staining of viral antigen with rabbit anti-MHV-A59 serum was carried out on paraffin-embedded sagittal sections from brains collected on day 5 postinfection from mice infected with SJHM-RA59, expressing wild-type JHM spike (a, b); SJHM-HR1, expressing JHM spike with three HR1 substitutions (c, d); or SJHM-L1114R, expressing the JHM spike with the L1114R substitution alone (e, f). Shown are regions of the olfactory bulbs (a, c, e) and the basal forebrain (d, f, g). The secondary antibody was TRITC-conjugated swine anti-rabbit antibody. Bars, 20 μm.

was less than 1.0 $\log_{10}$ unit. SJHM-L1114R replicated less efficiently than SJHM-RA59; however, the difference between the titer of infectious virus in the brains of mice infected with these two viruses at 5 days postinfection was not significant (two-tailed *t* test, $P < 0.06$ and $P < 0.11$ for each of the two SJHM-L1114R isolates). Thus, although there is a striking difference in virulence after in inoculation with these viruses, this difference cannot be explained by the extent of viral replication in the brains of infected animals.

To further investigate the attenuated phenotype of these mutants, we used indirect immunofluorescence to visualize viral antigen in the brains of SJHM-HR1- and SJHM-L1114R-infected animals. Brain sections were obtained from mice infected in with 5000 PFU of SJHM-RA59, SJHM-HR1, and SJHM-L1114R at 5 days postinfection. These sections were labeled with polyclonal antisera directed against MHV structural proteins and then detected using a biotin-avidin-labeled secondary antibody as described under Materials and methods. The difference in the patterns of viral antigen distribution observed in the brains of animals infected with SJHM-RA59 and the viruses expressing mutant spike was striking. The distribution of SJHM-RA59 viral antigen was widespread. Viral antigen was detected in olfactory bulbs, as well as in other regions of the brain, from the basal forebrain to the brain stem (Phillips et al., 1999). (Fig. 6 shows sections from the basal forebrain and the olfactory bulbs.) However, in mice infected with SJHM-HR1 or SJHM-L1114R, viral antigen was primarily detected in the mitral layer of the olfactory bulbs and in the adjacent glomerular and external plexiform layers (see below). Outside the olfactory bulbs, there were only occasional antigen-positive cells. The majority of antigen-positive cells looked morphologically similar to neurons. Thus, both mutants showed patterns of antigen distribution similar to OBLV60 (Pearce et al., 1994); this

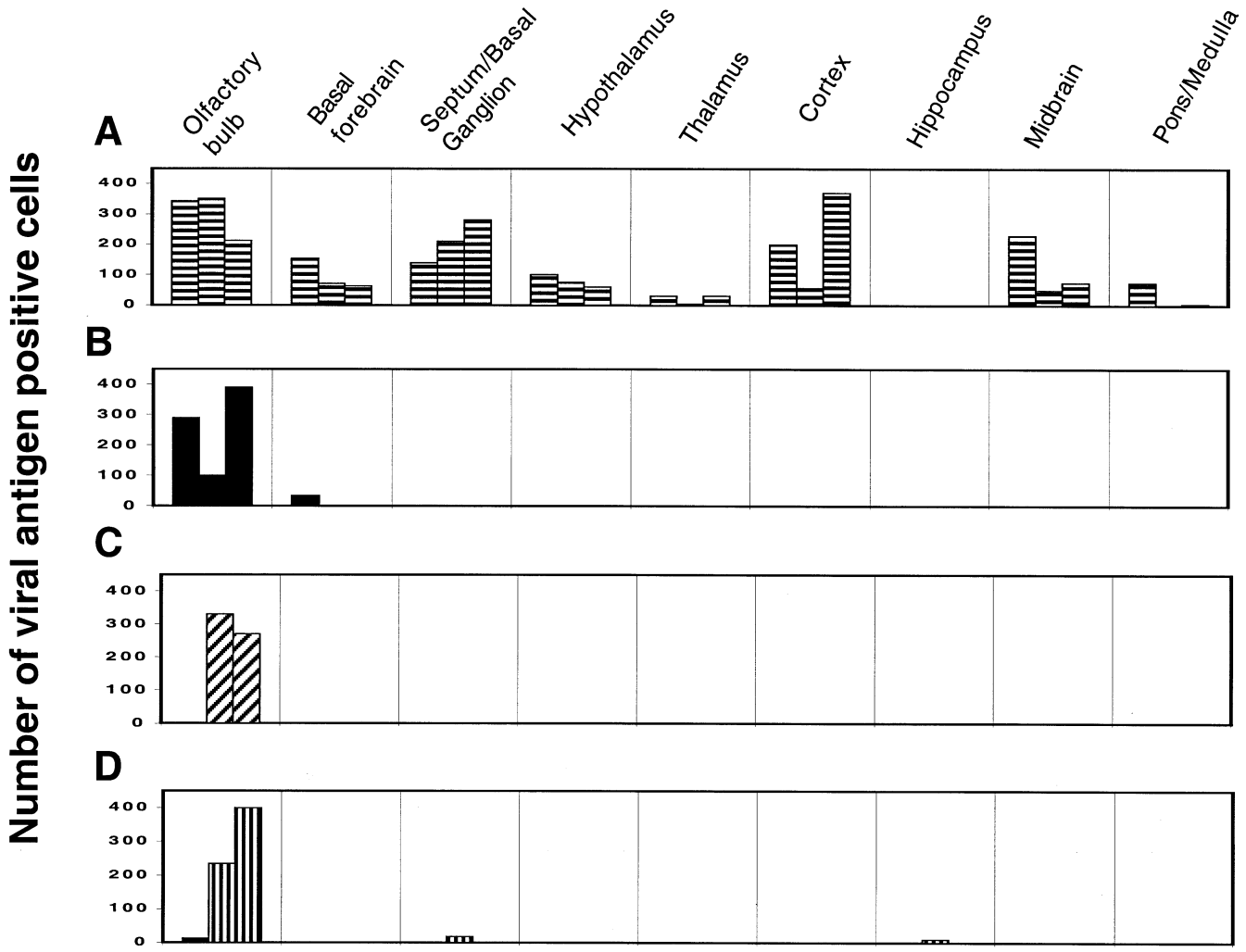

Fig. 7. Quantification of viral antigen expression in the brain. Indirect immunofluorescent staining of viral antigen was carried out on paraffin-embedded sagittal brain sections as described in Fig. 6 and under Materials and methods. The number of antigen-positive cells in each of the indicated regions of the brain at 5 days postinfection was counted under ×100 magnification. Three animals were examined per virus. For each mouse, the numbers from duplicate sections were averaged and plotted; thus the numbers shown are averages of six sections. (A) SJHM-RA59, expressing wild-type JHM spike; (B) SJHM-HR1 expressing the JHM spike with three HR1 substitutions; (C and D) two isolates of SJHM-L1114R, expressing the JHM spike with the L1114R substitution.

indicates that the L1114R substitution alone, as well as the three HR1 substitutions, is sufficient to restrict antigen expression to the olfactory bulbs.

We quantified the spread of SJHM-RA59, SJHM-HR1, and SJHM-L1114R antigen in the brain at day 5 postinfection by staining with immunofluorescent antibody and counting the number of antigen-positive cells in regions of the brain, including the olfactory bulbs and regions caudal to it (Fig. 7). From these data, it is clear that, while mice infected with all three viruses displayed viral antigen in the olfactory bulbs, only mice infected with SJHM-RA59 had significant numbers of infected cells in the other regions of the brain. By 7 days postinfection, the intense staining of SJHM-RA59 antigen in the olfactory bulbs had diminished and shifted to the pons and medullar regions (data not shown). Some SJHM-HR1 and SJHM-L1114R antigen staining was also observed in the more caudal regions of the brain, but it was of lower intensity and less extensive than SJHM-RA59 antigen.

There were some differences among the viruses in antigen spread within the olfactory bulbs as well. SJHM-RA59 antigen was found mostly in the mitral layer, often in cells with neuronal morphology; the glomerular layer of the olfactory bulbs was also labeled but less intensely than the mitral layer (data not shown). In addition, some SJHM-RA59 antigen was detected in deeper cell layers. The mutant virus antigen was found in abundance in the glomerular layer as well as in the mitral layer of the olfactory bulbs, and occasionally in the intervening external plexiform layer. There was less antigen present in deeper layers of the olfactory bulbs as compared with SJHM-RA59 antigen.

To further understand how the viruses expressing mutant spike proteins can replicate to similar titers as virus expressing wild-type JHM spike (SJHM-RA59), yet express mini-

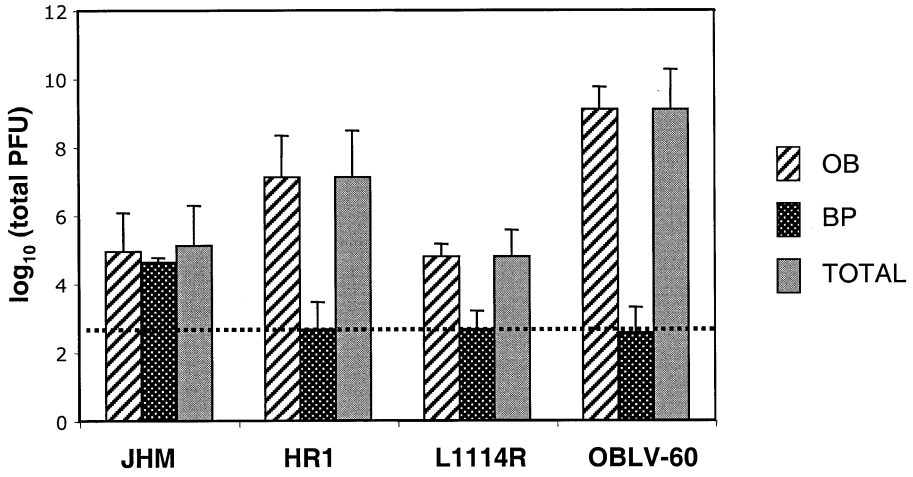

Fig. 8. Quantification of infectious virus in the olfactory bulbs and the brain parenchyma. Male 4-week-old C57B1/6 mice were inoculated intranasally with 5000 PFU of recombinant virus expressing wild-type JHM spike (JHM), with mutant spike proteins, either with three HR1 substitutions (HR1) or L1114R alone (L1114R) or with OBLV60. Mice were sacrificed 5 days postinfection and brains were harvested. Olfactory bulbs (OB) were separated from the rest of the brain parenchyma (BP). Both fractions were homogenized and infectious virus was quantified in each fraction by plaque assay. Also shown are the total brain titers, which are the sums of both fractions. Titers are expressed as the logarithmic mean of total PFU and standard deviations are represented as error bars. The limit of detection was 2.7 $\log_{10}$ (PFU) for the BP.

mal if any antigen outside of the olfactory bulbs, we quantified the amount of infectious virus in olfactory bulbs as compared with the rest of the brain (Fig. 8). In mice infected with either the single or the triple substitution HR mutants, the level of infectious virus within the olfactory bulbs was 2–5 $\log_{10}$ units greater than that in the rest of the brain. (The distribution of infectious virus was similar in brains from mice infected with OBLV60 (Fig. 8; Pearce et al., 1994).) For recombinant virus expressing wild-type JHM spike, approximately equal amounts of infectious virus were detected in the olfactory bulbs and the rest of the brain. Thus, for each virus, the amount of infectious virus present in the olfactory bulb as compared with the rest of the brain is consistent with level of viral antigen detected in each fraction (Fig. 6–8). For all viruses examined, the olfactory bulbs are an abundant source of infectious virus. The olfactory bulbs represent approximately 6% of the weight of the brain, yet even in animals infected with recombinant expressing wild-type spike, olfactory bulbs contain close to half the infectious virus.

Examination of inflammation in the CNS of mice infected with all three viruses, by staining of brain sections with hematoxylin and eosin, revealed pathologic changes consistent with acute meningoencephalitis. The relative intensity of inflammation varied from a few foci of perivascular cuffing to widespread foci with extensive parenchymal infiltration of lymphocytes and activated microglial cells with tissue necrosis. The observed levels of CNS inflammation were consistent with the levels of viral antigen-positive cells. By 5 days postinfection, inflammation was extensive for SJHM-RA59 in the olfactory bulbs and the rest of the brain; however, in SJHM-HR1- and SJHM-L1114R-infected brains, severe inflammation was found almost exclusively in the olfactory bulbs. By 7 days postinfection, inflammation was observed in more caudal regions of the brain for SJHM-HR1 and SJHM-L1114R; however, the extent and the intensity of inflammation were markedly less than that observed in the brains of mice infected with SJHM-RA59.

Discussion

Our goals were to determine (1) whether the three HR1 amino acid substitutions observed in the OBLV60 spike protein were indeed responsible for the low pH-dependent step in viral entry and/or the attenuated phenotype in vivo and (2) whether the attenuation and olfactory bulb localization observed for OBLV60 were linked to the fusion phenotype. Thus, we used targeted recombination to select viruses in a defined genetic background, differing from the parental virus only in the three mutations in HR1 of S2. These viruses express the JHM spike protein containing the three HR1 substitutions present in the OBLV60 spike (Q1067H, Q1094H, and L1114R). The genes other than the spike in these viruses were derived from MHV-A59. We had shown previously that the parental virus used for comparison for these experiments, SJHM- RA59, which contains the wild-type JHM spike, displays in vitro properties and the high neurovirulence phenotype exhibited by wild-type JHM (Phillips et al., 1999). We found that the recombinant virus, expressing the JHM spike with HR1 mutations. SJHM-HR1, displays similar phenotypes to OBLV60 (Gallagher et al., 1991; J.C. Tsai and S.R. Weiss, unpublished data). As described above, this includes sensitivity to lysosomotropic agents, inability to induce cell-to-cell fusion at neutral pH, as well as in vivo attenuation. Thus, with respect to the HR1 substitutions within JHM spike, the background

genes of the virus (MHV-A59 or JHM) do not influence the phenotypes that we have studied here.

Previous studies reported that the OBLV60 spike protein can induce cell-to-cell fusion if exposed to low pH for several hours (Gallagher et al., 1991). In our studies, neither SJHM-HR1 nor OBLV60 was able to induce cell-to-cell fusion, at neutral or low pH, even after incubation of infected cells at low pH for several hours. The difference between our observations and those of Gallagher et al. (1991) may be due to the way spike was expressed; Gallagher et al. (1991) utilized a vaccinia virus expression system, perhaps resulting in higher levels of cell-surface spike expression than those present during natural infection.

The acidic pH requirement for OBLV60 entry was demonstrated using a variety of lysosomotropic agents at various times during infection (Gallagher et al., 1991; Nash and Buchmeier, 1997). Similar to OBLV60, the recombinant virus expressing a spike with the three HR1 substitutions was nonfusogenic at neutral pH and its replication was sensitive to inhibition by lysosomotropic agents; this demonstrates that the HR1 substitutions identified in the OBLV60 spike are indeed responsible for the low pH requirement in viral entry. Our observations that SJHM-HR1 is highly attenuated in neurovirulence and restricted in spread from the olfactory bulbs into the more caudal areas of the brain allow us to conclude that the HR1 substitutions are responsible for the altered pathogenesis displayed by OBLV60 (Pearce et al., 1994).

To determine whether the L1114R substitution alone was responsible for any of the phenotypes of the SJHM-HR1, we selected recombinants with a spike containing only this substitution, SJHM-L1114R. We reasoned that this substitution could be responsible for only some of the phenotypes and thus that comparison of SJHM-L1114R with SJHM-HR1 would indicate whether the in vitro changes observed were responsible for and/or linked to the in vivo phenotypes. SJHM-L1114R induced syncytia at neutral pH, albeit at a lower level than SJHM- RA59; furthermore SJHM-L1114R was relatively resistant to the effects of lysosomotropic agents, but not quite as resistant as parental SJHM-RA59. Yet, the SJHM-L1114R viruses were attenuated and displayed antigen only in the olfactory bulbs. This demonstrates that the L1114R substitution is sufficient to cause altered pathogenesis and suggests that the low pH-dependent phenotype displayed by OBLV60 and SJHM-HR1 is not required for neuroattenuation and restricted spread within the CNS.

The HR domains of the MHV spike have been implicated in the mechanism of cell-to-cell fusion (Gallagher and Buchmeier, 2001; Krueger et al., 2001; Matsuyama and Taguchi, 2002b). By analogy with other viral spike proteins, such as HIV gp41 and influenza HA2, it is believed that conformational changes in spike, mediated by intramolecular heptad repeat interactions, are necessary to promote fusion through the insertion of the hydrophobic fusion peptide in the opposing cell's membrane (White, 1992; Carr et al., 1997; Singh et al., 1999). The three substitutions present in the SJHM-HR1 spike are found within HR1, downstream of the putative fusion peptide (Luo and Weiss, 1998). We have observed previously that uncharged-to-charged amino acid changes within HR1, such as L to R, can affect the ability of the MHV spike to induce cell-to-cell fusion despite the fact that such spike molecules are processed and delivered to the plasma membrane (Luo and Weiss, 1998). Gallagher et al. (1991) suggested that the acquisition of a titratable proton and/or positive charge, as a result of the Q-to-H substitutions within the OBLV60 spike HR1, could result in the requirement for a low pH (pH 6) environment for the activation of fusion. However for the OBLV60 spike and the spike proteins studied here, multiple substitutions were necessary for the low pH requirement for fusion; in a vaccinia virus based expression system, neither spike proteins with the L1114R alone nor proteins with both Q-to-H substitutions without L1114R could induce the altered fusion phenotype (Gallagher et al., 1991). Consistent with this, the L1114R substitution alone results in only a small decrease in the ability to induce cell-to-cell fusion at neutral pH and does not confer significant sensitivity to ammonium chloride (Figs. 3 and 4).

Substitutions at L1114 within the JHM spike (L1114R or L1114F) are particularly intriguing in that they have been reported in association with several mutant phenotypes. In addition to L1114R in the OBLV60 spike (Gallagher et al., 1991), substitutions at this residue have been identified in the spike of a monoclonal antibody resistant mutant (Wang et al., 1992) and a soluble receptor resistant mutant, srr7 (Saeki et al., 1997). The srr7 mutant (expressing a spike containing L1114F) demonstrated increased stability of the S1/S2 interaction, the loss of the ability to induce CEACAM-independent fusion (Taguchi and Matsuyama, 2002), and altered interactions with CEACAM1^{b} as well as soluble receptor (Matsuyama and Taguchi, 2002a, b). Similarly, OBLV60 exhibits increased thermostability (M. Buchmeier, personal communication) and loss of the ability to induce CEACAM-independent fusion (T. Gallagher, personal communication). The recombinant virus expressing L1114R alone (described in this article) is also unable to induce CEACAM-independent cell-to-cell fusion (data not shown). Finally, recombinant viruses expressing A59/JHM chimeric spikes were also neuroattenuated, thermostable, and unable to induce receptor independent cell-to-cell fusion (Tsai and Weiss, 2001; Tsai et al., 2003). Thus, these data are consistent with the observation that high thermolability, the ability to induce receptor-independent fusion, and the propensity to dissociate from receptor are associated with high neurovirulence and rapid spread in the CNS and relatively less efficient replication in cultured cells, displayed by JHM (Krueger et al., 2001; Gallagher and Buchmeier, 2001; Phillips et al., 1999).

Interestingly, the restriction of antigen expression to the olfactory bulbs did not result in a difference in brain titers between mutant and wild-type recombinant viruses. By day

5, both SJHM-RA59 and mutant viruses (SJHM-HR1 and SJHM-L1114R) replicated to much higher titers, per gram of tissue in the olfactory bulb, as compared with the rest of the brain (Fig. 8). Thus, the titer of infectious virus in the olfactory bulbs represents a large fraction of total virus in the brain and the ability of virus to replicate in the olfactory bulb is sufficient to achieve a high titer. Furthermore, the observation that the recombinant viruses expressing mutant spikes replicated to similar titers as wild-type is consistent with previous observations that the level of replication of MHV in the CNS is not necessarily reflective of the neurovirulence level (Phillips et al., 1999).

It is plausible that the L1114R (or F) substitution alters the structure of the spike protein such that the mutant spike protein is less fit than wild-type and thus viral spread is impaired or slowed down compared to virus expressing wild-type JHM spike. Alternatively, it is possible that the neurons of the olfactory bulbs are different from other neurons (perhaps, for example, in receptor expression) and that viruses with the L1114R substitution cannot replicate in cells outside the olfactory bulbs. However, this is not an absolute restriction, because at later times postinfection, increased numbers of infected cells are detected outside of olfactory bulbs (data not shown). Consistent with this observation, OBLV60 can spread beyond the olfactory bulbs when the immune response is compromised (Pearce et al., 1994). Thus, it is likely that the differences in the efficiency of replication between the mutant and the wild-type recombinant viruses in the CNS give the immune response an advantage that restricts spread sooner and more efficiently than for wild-type virus.

Materials and methods

Cells and viruses

Murine L2, 17C1-1 and DBT cells, and feline FCWF cells were maintained in tissue culture flasks in Dulbecco's minimal essential medium (DMEM) supplemented with 10% fetal bovine serum (FBS) (Gibco-BRL). JHM and OBLV60 were obtained from Dr. M. Buchmeier (La Jolla, CA). (The JHM isolate we are using has previously been referred to in the literature as MHV-4 (Dalziel et al., 1986; Gallagher et al., 1991). The coronavirus nomenclature committee has decided to eliminate the use of the MHV-4 nomenclature; thus, all isolates of JHM are referred to simply as JHM.) We have used two independently selected recombinant viruses containing the JHM spike gene with the rest of the genes derived from MHV-A59. These were called S_4R22 and S_4R29 in previous publications (Navas et al., 2001; Phillips et al., 2001, 2002). These two isolates behave identically and will be referred to collectively as SJHM-RA59, that is, a recombinant A59 with the spike gene derived from JHM, SJHM-RA59 serves as the recombinant wild-type virus. fMHV (obtained from Paul Masters, Albany, NY) is a recombinant virus, which expresses the ectodomain of the feline infectious peritonitis (FIPV) S gene in the MHV-A59 background (Kuo et al., 2000; Ontiveros et al., 2001).

Plasmids and PCR mutagenesis

pSwt, encoding the wild-type JHM (MHV-4) spike in pGEM4Z, was obtained from Dr. Michael Buchmeier (Gallagher et al., 1991); pSwt was further modified to construct pGEM4Z-S4. *Avr*II and *Sbf*1 restriction sites were created at the 5′ and 3′ ends of the spike gene, as described previously (Phillips et al., 1999). pMH54-S4 was subsequently constructed by the ligation of the JHM spike gene (excised from pGEM4Z-S4 by digestion with *Avr*II/*Sbf*I) into *Avr*II/*Sbf*I-cleaved pMH54, in place of the MHV-A59 spike gene (Phillips et al., 1999). The plasmid pS-OBL60 (obtained from Michael J. Buchmeier) is a pGEM4Z plasmid, which contains the spike gene of the OBLV60 virus (Fig. 1).

The spike gene of OBLV60 was amplified from pS-OBLV60 by PCR using the primers JJ3 and A59-9 (Table 1; Phillips et al., 1999). The amplified OBLV60-fragment was digested with *Bam*HI and *Pst*I and a 1166 base pair fragment, encoding the three mutations in HR1 (Q1067H, Q1094H, and L1114R), was subcloned into the corresponding site in pGEM4Z-S4. The resulting plasmid was called pGEM-OBLV60(HRImut). The *Avr*II/*Sbf*I fragment from this plasmid, containing the mutant spike gene, was subcloned into pMH54-S4 to yield pMH-OBLV60(HR1mut). The spike gene encoded in pMH-OBLV60(HR1mut) was sequenced to verify that the three target mutations, and no additional mutations, were introduced. PCR- mediated mutagenesis to introduce the L1114R substitution was carried out in pG-MHV4S, a derivative of pGEM4Z-S4 that contains the full start signal upstream of the *Avr*II site. The mutagenic primer JFSL1114R2, which encodes the L1114R substitution (generated by a C-to-T at nucleotide 3340 and a T-to-C at nucleotide 3342 of the spike gene), and JRS-SBF (Table 1) were used to amplify the 3′ end of the S gene. This fragment was digested with *Hin*cII and *Sbf*I and subcloned into pG-MHV4S to generate pG-L1114R. After verifying the sequences in the amplified region, the *Avr*II/*Sbf*I fragment of the spike gene was ligated into pMH54, generating pMH-L1114R.

Targeted RNA recombination

Targeted RNA recombination was used to generate the recombinant viruses (Kuo et al., 2000; Phillips et al., 2001). The recombinant viruses express the JHM spike with the rest of the background genes derived from A59. Synthetic capped RNAs were synthesized by linearizing the plasmids pMH54-S4, pMH-OBLV60(HR1mut), and pMH-SJHM-L1114R using the restriction enzyme *Pac*I and then transcribing with T7 polymerase (Ambion). Recombination was carried out between the donor RNA and the recipient virus,

Table 1
Primers used for PCR mutagenesis

Primer	Sequence (5′ to 3′)	Polarity	Genome location
A59-9	TCTGATGTTGGCTTTGTCGAGG	Positive	2503–2824 of spike gene
JJ3	gcggatccaagtCCtGcAGgGGCTGTGATAGTCAATCCTCATGAGA	Negative	Intergenic region between S and 4a
JFSL1114R2	GCAGGTTAACTGCACTTAATGCGTATATATCCAAGCAATTCAGTGATAGTA	Positive	3302–3352 of spike gene
JRS-SBF	CGTAAGTCCTGCAGGGGCTGTGATA	Negative	Intergenic region between S and 4a

[a] Nonviral sequences, used to introduce restriction sites or new codons, are indicated by lower case.
[b] The locations are designated by nucleotide positions in the spike (S) open reading frame (ORF).

fMHV in feline FCWF cells (Kuo et al., 2000; Phillips et al., 2001), and the recombinants selected by their ability to replicate in murine L2 cells; individual isolates were purified by two rounds of plaque purification on L2 cells. Two independently selected recombinant viruses for each mutant were chosen for further study. The pair expressing all three mutations in HR1 were called SJHM-HR1-R120 and SJHM-HR1-R121 and are referred to collectively as SJHM-HR1. The pair expressing L1114R only were called SJHM-L1114R-R300 and SJHM-L1114R-R301 and are referred to collectively as SJHM-L1114R or when data is shown for each isolate as SJHM-L1114R-A and SJHM-L1114R-B, respectively. (We have shown in the past that pairs of independently selected recombinant viruses with the same mutations exhibit identical phenotypes (Leparc-Goffart et al., 1998; Phillips et al., 1999, 2001).)

All recombinant MHV spike genes were sequenced in full, using previously described primers (Leparc-Goffart et al., 1997; Phillips et al., 1999) and compared to the published JHM spike gene sequence (Parker et al., 1989). Our wild-type JHM spike gene has in addition one silent mutation at nucleotide 3990 (Gallagher et al., 1991) and an L255A substitution (Phillips et al., 1999). The spike of SJHM-HR1-R120 contained no additional amino acid substitutions; however, the spike of SJHM-HR1-R121 did have another amino acid substitution, N78D. Thus we show data for SJHM-R120 for all of the experiments. Spike protein expressed by SJHM- L1114R-R300 and SJHM-L1114R-R301 had no additional substitutions.

Virus replication in vitro

One-step replication curves were carried out in L2 cell monolayers and virus was titered by plaque assay on L2 cells, as previously described (Phillips et al., 2001). To investigate the inhibitory effects of lysosomotropic agents on virus replication, L2 cells were pretreated with medium containing either 20 mM ammonium chloride (Sigma) or 40 mM chloroquine (Sigma) for 1 h prior to infection. Cells were infected at an m.o.i. of 1 PFU/ cell at 37°C for 1 h, and the inoculum was removed. The cells washed with phosphate-buffered saline (PBS) and medium containing the same concentrations of chloroquine or ammonium chloride was added back. At the indicated times postinfection, cells were lysed and viral titers were determined by plaque assay (Phillips et al., 2001). (Only the data for ammonium chloride treatment are shown.)

Cell-to-cell fusion assay

L2 monolayers were infected at a multiplicity of infection of 1 PFU per cell and incubated in DMEM-10% FBS at 37°C. At 7 or 9 h postinfection, the monolayers were washed with PBS and fixed with 2% paraformaldehyde (Sigma Chemical Co., St. Louis, MO). Syncytium formation was quantified by counting the number of nuclei in syncytium and the number of single nuclei per field at $\times 200$ magnification. A total of 10 fields, of approximately 200 nuclei each and from duplicate wells, were counted per virus. The average and the standard deviation of the percentage of cells that were fused were calculated. The percentage of fusion was calculated by the following formula: % fusion = nuclei in syncytium/total number of nuclei per field.

Infections in mice

Virus-free, male 4-week-old C57BL/6 mice from NCI were used for all animal experiments. Viruses were diluted into PBS containing 0.75% bovine serum albumin. Mice were anesthetized with isofluorane (IsoFlo, Abbott Laboratories, North Chicago, IL). For intracranial inoculations, 20 μl of diluted virus was injected into the left cerebral hemisphere. For intranasal inoculation, 5 μl of the diluted virus was introduced into each nostril. For mock-infected controls, an uninfected cell lysate at a comparable dilution was used for inoculation. Virulence was measured in lethal dose $(LD)_{50}$ units, the amount of virus needed to kill 50% of the mice. Mice were inoculated ic or in with serial dilutions of virus, five mice per dilution, and were examined for signs of disease or death on a daily basis up to 28 days postinfection. LD_{50} values were calculated by the Reed–Muench method (Reed and Muench, 1938; Lavi et al., 1984).

To measure the kinetics of virus replication, mice were infected in. Groups of mice (three to four mice) were sacrificed at 1, 3, 5, and 7 days postinfection and perfused with

10 ml of PBS, prior to removal of the brain. The left half of the brain (cut sagittally) was placed directly into 2 ml of isotonic saline with 0.16% gelatin for virus titer determination. The right half of the brain was stored in 8–10 ml of 10% phosphate-buffered formalin for histology and viral antigen staining (see below). All organs were weighed and stored at −80°C until titers were determined. Organs were homogenized and virus titers were measured by plaque assay on L2 cell monolayers. For the quantification of virus in the olfactory bulbs and the rest of the brain (Fig. 8), olfactory bulbs were separated from the rest of the brain parenchyma and each fraction was placed into gel saline, homogenized, and titered for infectious virus by plaque assay on monolayers of L2 cells.

Histology and immunofluorescence

The formalin fixed tissue (right half of the brain, see above) was embedded in paraffin, sectioned, and stained with hematoxylin and eosin (H&E) for histological analysis, or left unstained for analysis of viral antigen distribution by indirect immunofluorescence. Following removal of the paraffin, slides were transferred to a 0.01 M citric acid bath at >96°C for 15 min, allowed to cool to room temperature, and then washed in double-deionized water. Sections were blocked with 1.5% goat serum in 0.1 M Tris–HCl and 1% Triton X-100 for up to 1 h, incubated for 2 h with UV13, a polyclonal antiserum raised against MHV-A59 (obtained from Mark Denison, Vanderbilt University). The subsequent incubation with the secondary antibody, biotin-conjugated goat anti-rabbit immunoglobulin (Vector Labs, CA) for 1 h, was followed by incubation with tetramethylrhodamine-5 (and 6) isothiocyanate (TRITC)-conjugated goat anti-rabbit immunoglobulin (Dako) for 30 min. All incubations were carried out at 37°C in a humidified chamber and were followed by extensive washes in PBS. Sections were photographed as in Fig. 6. Alternatively, individual regions of the brain were observed and antigen-positive cells were counted in each region as in Fig. 7.

Acknowledgments

This work was supported by Public Health Service Grants NS-30606 and NS-21954 (S.R.W.) and National Multiple Sclerosis Society Grant RG2615 (E.L.). J.C.T. was supported in part by funds from Public Health Service Grant NIH-T32-AI-07325.

References

Barnett, E.M., Cassell, M.D., Perlman, S., 1993. Two neurotropic viruses, herpes simplex virus type 1 and mouse hepatitis virus, spread along different neural pathways from the main olfactory bulb. Neuroscience 57, 1007–1125.

Carr, C.M., Chaudhry, C., Kim, P.S., 1997. Influenza hemagglutinin is spring-loaded by a metastable native conformation. Proc. Natl. Acad. Sci. USA 94, 14306–14313.

Dalziel, R.G., Lampert, P.W., Talbot, P.J., Buchmeier, M.J., 1986. Site-specific alteration of murine hepatitis virus type 4 peplomer glycoprotein E2 results in reduced neurovirulence. J. Virol. 59, 463–471.

DeGroot, R.J., Luytjes, W., Horzinek, M.C., van der Zeijst, B.A.M., Spaan, W.J.M., Lenstra, J.A., 1987. Evidence for a coiled-coil structure in the spike proteins of coronaviruses. J. Mol. Biol. 196, 963–966.

Dveksler, G.S., Pensiero, M.N., Cardellichio, C.B., Williams, R.K., Jiang, G.S., Holmes, K.V., Dieffenbach, C.W., 1991. Cloning of the mouse hepatitis virus (MHV) receptor: expression in human and hamster cell lines confers susceptibility to MHV. J. Virol. 65, 6881–6891.

Frana, M.F., Behnke, J.N., Sturman, S., Holmes, K.V., 1985. Proteolytic cleavage of the E2 glycoprotein of murine coronavirus: host-dependent differences in proteolytic cleavage and cell fusion. J. Virol. 56, 912–920.

Gallagher, T.M., Buchmeier, M.J., 2001. Coronavirus spike proteins in viral entry and pathogenesis. Virology 279, 371–374.

Gallagher, T.M., Escarmis, C., Buchmeier, M.J., 1991. Alteration of pH dependence of coronavirus-induced cell fusion: effect of mutations in the spike glycoprotein. J. Virol. 65, 1916–1928.

Hsue, B., Masters, P.S., 1998. An essential secondary structure in the 3′ untranslated region of the mouse hepatitis virus genome. Adv. Exp. Med. Biol. 440, 297–302.

Krueger, D.K., Kelly, S.M., Lewicki, D.N., Ruffolo, R., Gallagher, T.M., 2001. Variations in disparate regions of the murine coronavirus spike protein impact the initiation of membrane fusion. J. Virol. 75, 2792–2802.

Kubo, H., Yamada, Y.K., Taguchi, F., 1994. Localization of neutralizing epitopes and the receptor-binding site within the amino-terminal 330 amino acids of the murine coronavirus spike protein. J. Virol. 68, 5403–5410.

Kuo, L., Godeke, G.J., Raamsman, M.J., Masters, P.S., Rottier, P.J., 2000. Retargeting of coronavirus by substitution of the spike glycoprotein ectodomain: crossing the host cell species barrier. J. Virol. 74, 1393–1406.

Lavi, E., Gilden, D.H., Wroblewska, Z., Rorke, L.B., Weiss, S.R., 1984. Experimental demyelination produced by the A59 strain of mouse hepatitis virus. Neurology 34, 597–603.

Lavi, E., Murray, E.M., Makino, S., Stohlman, S.A., Lai, M.M.C., Weiss, S.R., 1990. Determinants of coronavirus MHV pathogenesis are localized to 3′ portions of the genome as determined by ribonucleic acid-ribonucleic acid recombination. Lab. Investig. 62, 570–578.

Leparc-Goffart, I., Hingley, S.T., Chua, M.M., Jiang, X., Lavi, E., Weiss, S.R., 1997. Altered pathogenesis of a mutant of the murine coronavirus MHV-A59 is associated with a Q159L amino acid substitution in the spike protein. Virology 239, 1–10.

Leparc-Goffart, I., Hingley, S.T., Chua, M.M., Phillips, J., Lavi, E., Weiss, S.R., 1998. Targeted recombination within the spike gene of murine coronavirus mouse hepatitis virus-A59: Q159 is a determinant of hepatotropism. J. Virol. 72, 9628–9636.

Lewicki, D.N., Gallagher, T.M., 2002. Quaternary structure of coronavirus spikes in complex with carcinoembryonic antigen-related cell adhesion molecule cellular receptors. J. Biol. Chem. 277, 19727–19734.

Luo, Z., Matthews, A.M., Weiss, S.R., 1999. Amino acid substitutions within the leucine zipper domain of the murine coronavirus spike protein cause defects in oligomerization and the ability to induce cell-to-cell fusion. J. Virol. 73, 8152–8159.

Luo, Z., Weiss, S.R., 1998. Roles in cell-to-cell fusion of two conserved hydrophobic regions in the murine coronavirus spike protein. Virology 244, 483–494.

Matsuyama, S., Taguchi, F., 2002a. Receptor-induced conformational changes of murine coronavirus spike protein. J. Virol. 76, 11819–11826.

Matsuyama, S., Taguchi, F., 2002b. Communication between S1N330 and a region in S2 of murine coronavirus spike protein is important for

virus entry into cells expressing CEACAM1b receptor. Virology 295, 160–171.

Nash, T.C., Buchmeier, M.J., 1997. Entry of mouse hepatitis virus into cells by endosomal and nonendosomal pathways. Virology 233, 1–8.

Navas, S., Seo, S.H., Chua, M.M., Sarma, J.D., Lavi, E., Hingley, S.T., Weiss, S.R., 2001. Murine coronavirus spike protein determines the ability of the virus to replicate in the liver and cause hepatitis. J. Virol. 75, 2452–2457.

Ontiveros, E., Kuo, L., Masters, P.S., Perlman, S., 2001. Inactivation of expression of gene 4 of mouse hepatitis virus strain JHM does not affect virulence in the murine CNS. Virology 289, 230–238.

Parker, S.E., Gallagher, T.M., Buchmeier, M.J., 1989. Sequence analysis reveals extensive polymorphism and evidence of deletions within the E2 glycoproteins of several strains of murine hepatitis virus. Virology 173, 664–673.

Pearce, B.D., Hobbs, M.V., McGraw, T.S., Buchmeier, M.J., 1994. Cytokine induction during T-cell-mediated clearance of mouse hepatitis virus from neurons in vivo. J. Virol. 68, 5483–5495.

Phillips, J.J., Chua, M., Rall, G.F., Weiss, S.R., 2002. Murine coronavirus spike glycoprotein mediates degree of viral spread, inflammation and virus-induced immunopathology in the central nervous system. Virology 301, 109–120.

Phillips, J.J., Chua, M., Seo, S.H., Weiss, S.R., 2001. Multiple regions of the murine coronavirus spike glycoprotein influence neurovirulence. J. Neurovirol. 7, 421–431.

Phillips, J.J., Chua, M.M., Lavi, E., Weiss, S.R., 1999. Pathogenesis of chimeric MHV4/MHV-A59 recombinant viruses: the murine coronavirus spike protein is a major determinant of neurovirulence. J. Virol. 73, 7752–7760.

Reed, L.J., Muench, H., 1938. A simple method of estimating fifty percent points. Am. J. Hyg. 27, 493–497.

Saeki, K., Ohtsuka, N., Taguchi, F., 1997. Identification of spike protein residues of murine coronavirus responsible for receptor-binding activity by use of soluble receptor-resistant mutants. J. Virol. 71, 9024–9031.

Singh, M., Berger, B., Kim, P.S., 1999. LearnCoil-VMF: computational evidence for coiled-coil-like motifs in many viral membrane-fusion proteins. J. Mol. Biol. 290, 1031–1041.

Taguchi, F., Matsuyama, S., 2002. Soluble receptor potentiates receptor-independent infection by murine coronavirus. J. Virol. 76, 950–958.

Tsai, J.C., Weiss, S.R., 2001. In vitro properties and pathogenesis of A59/MHV4 chimeric mouse hepatitis viruses. Adv. Exp. Med. Biol. 494, 169–172.

Tsai, J.C., Zelus, B.D., Holmes, K.V., Weiss, S.R., 2003. The N-terminal domain of the murine coronavirus spike glycoprotein determines the CEACAM1 receptor specificity of the virus strain. J. Virol. 77, 841–850.

Wang, F.I., Fleming, J.O., Lai, M.M., 1992. Sequence analysis of the spike protein gene of murine coronavirus variants: study of genetic sites affecting neuropathogenicity. Virology 186, 742–749.

White, J., 1992. Membrane fusion. Science 258, 917–924.

Zelus, B.D., Schickli, J.H., Blau, D.M., Weiss, S.R., Holmes, K.V., 2003. Conformational changes in the spike glycoprotein of murine coronavirus are induced at 37°C by soluble murine CEACAM1 receptor glycoproteins or by pH 8. J. Virol. 77, 830–840.